

Supporting Information for:

## **Rapid, multiparameter profiling of cellular secretion using silicon photonic microring resonator arrays**

Matthew S. Luchansky & Ryan C. Bailey\*

*Department of Chemistry, University of Illinois at Urbana-Champaign*

*600 South Mathews Avenue, Urbana, Illinois 61801*

\*Email: [baileyr@illinois.edu](mailto:baileyr@illinois.edu); Phone: (217) 333-0676

### **Table of Contents:**

Experimental Details.....	S2
Multiplexed capture antibody functionalization & covalent conjugation to microrings.....	S2
Isolation of PBMCs from whole blood.....	S3
Negative selection of naïve CD4 <sup>+</sup> T cells from PBMCs.....	S3
T cell activation and differentiation protocols.....	S4
Method for sampling cell culture aliquots.....	S5
Initial slope data analysis and cytokine quantitation through calibration.....	S5
Paired difference <i>t</i> -test for comparing cytokine secretion levels.....	S6
Figure S1. Ring resonator chip micrograph with microfluidic schematic.....	S7
Figure S2. Real-time plot of 4-plex capture antibody loading.....	S7
Figure S3. Negative control experiment for one-step sandwich assay.....	S8
Figure S4. Calibration curves for quantitative multiplexed analysis.....	S8
Figure S5. 4-plex cytokine temporal secretion profile for Jurkat T cells.....	S9
Figure S6. ELISA validation of temporal secretion study.....	S9
Figure S7. T cell differentiation schematic and cytokine secretion signatures.....	S10
Figure S8. Primary T cell microscope images: Time-course study.....	S11
Figure S9. Real-time multiplexed cytokine binding for Th0/Th1/Th2 culture aliquots.....	S12
Figure S10. Effect of proteases on real-time binding curves.....	S13
Figure S11. Cytokine temporal secretion profiles for Th0, Th1, and Th2 subsets.....	S14
Table S1. Calibration standard cocktails.....	S15
Table S2. Limits of detection: One-step sandwich.....	S16
Supporting Information References.....	S17

## Experimental Details

### Multiplexed capture antibody functionalization and covalent conjugation to microrings

Prior to functionalization, chips were cleaned by a 30-s immersion in piranha solution (3:1 H<sub>2</sub>SO<sub>4</sub>:30% H<sub>2</sub>O<sub>2</sub>)\* followed by a water rinse and drying in a nitrogen stream. After a 30-min sonication in 100% ethanol, chips were dried in a nitrogen stream and spotted with 1 mg mL<sup>-1</sup> HyNic silane (3-*N*-((6-*N*-isopropylidene-hydrazino))nicotinamide)propylthriethoxysilane, SoluLink) in 95% ethanol/5% dimethyl-formamide (DMF) for a 20-min incubation at room temperature to install a hydrazine moiety. Following silanization, chips were sonicated for 15 min in 100% ethanol to remove physisorbed silane. After drying in a nitrogen stream, chips were loaded into a previously described fluidic cell<sup>1</sup> with a custom 4-channel fluidic gasket<sup>2</sup> (Scarpati Technical Services/RMS Laser) to direct antibody solution flow to defined groups of 4-5 rings each (Figure S1).

Capture antibodies [anti-IL-2 clone 5344.111 (555051, BD Biosciences); anti-IL-4 clone 8D4-8 (14-7049, eBioscience); anti-IL-5 clone TRFK5 (14-7052, eBioscience); anti-TNF $\alpha$  clone MAb1 (14-7348, eBioscience)] were first buffer-exchanged into 100 mM phosphate-buffered saline (PBS) pH 7.4 with Zeba spin desalting columns (7k molecular weight cutoff, Fisher Scientific). In separate reaction vials, lysine residues on the 4 capture antibodies were functionalized with aldehyde moieties by reacting 0.5 mg mL<sup>-1</sup> antibody with a 10-fold molar excess of succinimidyl-4-formyl benzoate (S-4FB, SoluLink, 0.5 mg mL<sup>-1</sup> in DMF) for 2 h at room temperature. After another buffer exchange into 100 mM PBS pH 7.4 to remove excess S-4FB and DMF, the antibody solutions were diluted to 30  $\mu$ g mL<sup>-1</sup> in 100 mM PBS pH 6 with 50 mM aniline. The capture antibody-4FB conjugates were flowed over the chip using the previously described fluidics controlled by a multi-channel programmable syringe pump (BS-9000-8, Brintree Scientific Inc.) operated in withdraw mode at 2  $\mu$ L min<sup>-1</sup>. Covalent antibody attachment by hydrazone bond formation between the hydrazine silane surface and aldehyde-modified antibodies was catalyzed by aniline<sup>3</sup> in the running buffer to allow full surface coverage after ~30 min. The antibody

---

\* Caution! Piranha solutions are extraordinarily dangerous, reacting explosively with trace quantities of organics.

loading was observed in real time (Figure S2) until 200-400 pm of net antibody shift was observed ( $\sim 5$  ng/mm<sup>2</sup> surface coverage<sup>4</sup>). Control rings covered by the fluidic gasket were monitored to ensure that they were not exposed to any antibody solution. After multiplexed antibody functionalization, chips were blocked overnight at 4 °C in StartingBlock PBS buffer (37538, Fisher Scientific). Functionalized chips can be stored refrigerated for up to a week prior to use.

### **Isolation of PBMCs from whole blood**

Primary blood mononuclear cells (PBMCs) were isolated from whole blood by Ficoll-Paque Plus (GE Healthcare) density gradient centrifugation according to the manufacturer's instructions. In brief, 18 mL whole blood was diluted 1:1 with 2% FBS in sterile PBS (Ca/Mg-free), divided into four 9-mL aliquots, and carefully layered onto four 15-mL tubes containing Ficoll (4.5 mL) with a serological pipette, taking care to minimize mixing. The layered blood on Ficoll was then spun at 400 g for 30 min (with the rotor brake off) to create a density gradient, from which the middle buffy coat layer of PBMCs was extracted by careful pipetting. The PBMCs from all 4 tubes were combined, washed with 2% FBS in sterile PBS, and spun at 500 g for 5 min to pellet cells. PBMCs were then resuspended in 5 mL 2% FBS in sterile PBS and counted ( $\sim 20 \times 10^6$  PBMCs from 18 mL whole blood). Cells were then spun down again and resuspended in 0.4 mL 2% FBS in sterile PBS to give  $\sim 50 \times 10^6$  cells/mL for naïve CD4<sup>+</sup> T cell enrichment by negative selection.

### **Negative selection of naïve CD4<sup>+</sup> T cells from PBMCs**

Negative selection was performed using magnetic bead separation with the EasySep naïve CD4<sup>+</sup> T cell enrichment kit (19115, Stem Cell Technologies) according to the manufacturer's instructions. In brief, a cocktail of antibodies against cell surface markers indicative of memory T cells (CD45RO<sup>+</sup>)<sup>5</sup> and

other cell types are added prior to incubation with magnetic particles that label the unwanted cells. By placing the tube inside the EasySep magnet, unwanted cells are held against the side of the tube, and the naïve CD4<sup>+</sup> T cells that remain in solution are decanted into another tube. A second round of magnetic separation was performed on the same cells to improve cell recovery. Only naïve (CD4<sup>+</sup>CD45RA<sup>+</sup>) T cells (2-3 x 10<sup>6</sup>) remain after magnetic negative selection. The negative selection process was verified by flow cytometry analysis (BD Biosciences LSR II) before and after magnetic bead separation using APC-conjugated anti-human CD4 (clone RPA-T4, 17-0049, eBioscience), PE-conjugated anti-human CD45RO (clone UCHL1, 12-0457, eBioscience), and FITC-conjugated anti-human CD45RA (clone JS-83, 11-9979, eBioscience). It was observed that the CD4<sup>+</sup>/CD45RO<sup>+</sup> (memory) population disappeared after separation, leaving only the CD4<sup>+</sup>/CD45RA<sup>+</sup> (naïve) population. The naïve CD4<sup>+</sup> T cells were spun down and resuspended in T cell media: RPMI 1640 (ATCC) supplemented with 10% FBS, 4.5 g L<sup>-1</sup> glucose, 2 mM L-glutamine, 10 mM HEPES, 1 mM sodium pyruvate, 1.5 g L<sup>-1</sup> sodium bicarbonate, penicillin and streptomycin (100 U mL<sup>-1</sup> each), prepared by the School of Chemical Sciences Cell Media Facility at the University of Illinois at Urbana-Champaign.

### **T cell activation and differentiation protocols**

Three wells of a 24-well plate were coated for primary T cell activation with 10 µg mL<sup>-1</sup> anti-CD3 (clone OKT3, 16-0037, eBioscience) and 10 µg mL<sup>-1</sup> anti-CD28 (clone CD28.2, 16-0289, eBioscience) in sterile PBS (1 mL per well) for 4 h at room temperature (or 8 h at 4 °C). The 3 wells (1 each for Th0, Th1, and Th2 differentiation) were rinsed twice with cell media prior to seeding naïve CD4<sup>+</sup> T cells at 2 x 10<sup>6</sup> cells mL<sup>-1</sup> (500 µL) per well. All 3 naïve T cell cultures were activated for proliferation and differentiation to Th0 (Figure S7) by adding 20 ng mL<sup>-1</sup> IL-2 (14-8029, eBioscience). Nothing more was added to the Th0 well. To direct Th1 differentiation, 20 ng mL<sup>-1</sup> IL-12 (148129, eBioscience) and 5 µg mL<sup>-1</sup> anti-IL-4 (clone MP4-25D2, 13-7048, eBioscience) were added to the Th1 well in addition to IL-

2. For Th2 differentiation, 20 ng mL<sup>-1</sup> IL-4 (34-8049, eBioscience), 5 μg mL<sup>-1</sup> anti-IFNγ (clone 4S.B3, 14-7319, eBioscience), and 5 μg mL<sup>-1</sup> anti-IL-10 (clone JES3-9D7, 14-7108, eBioscience) were added to the Th2 well in addition to IL-2. Cells were activated and differentiated in a cell incubator (37 °C; 5% CO<sub>2</sub>; 70% relative humidity).

### **Method for sampling cell culture aliquots**

After 0, 6, 12, 24, or 48 h of stimulation, cell aliquots (400-500 μL) were withdrawn from the wells. The cell culture aliquots were spun at 500 g for 5 min to pellet the cells, and ~400 μL cell-free supernatant was obtained for each aliquot. A cocktail of protease inhibitors (aprotinin, bestatin, E-64, leupeptin, and pepstatin A; P 1860, Sigma-Aldrich) in DMSO were added at 1:500 to all cell culture aliquots to prevent protease activity on secreted cytokines during storage. All aliquots were stored at -20 °C for up to 24 h prior to ring resonator analysis. Prior to analysis, cell aliquots were thawed, spiked with 1 μg mL<sup>-1</sup> each of anti-IL-2, anti-IL-4, anti-IL-5, and anti-TNFα as described previously, and treated a second time with protease inhibitors (1:500, for 1:250 total). Protease inhibitors were necessary to prevent degradation of blocking proteins and capture antibodies on the ring resonators that caused a downward sloping background (Figure S10).

### **Initial slope data analysis and cytokine quantitation through calibration**

The initial slope, which is proportional to concentration under mass-transport limiting analysis conditions<sup>1</sup>, was measured for each ring upon addition of cytokines pre-incubated with detection antibodies (Figure 1c). Specifically, 5 min of real-time binding data for each ring was fit with a linear regression for each standard and unknown sample. Four individual cytokine calibration curves were constructed for each experiment based on the average initial slope for the set of rings specific for a

particular cytokine. All signals were corrected for non-specific binding by subtracting the initial slope for a single control ring (not coated with an anti-cytokine capture antibody). The average control ring-corrected initial slope was plotted against concentration and well-fit with a linear regression (all  $R^2 \geq 0.990$ ) to obtain a calibration plot for each cytokine (Figure 3a; Figure S4). In this way, calibration curves for all 4 cytokines assayed were generated from the same series of multiplexed calibration standards. Initial slopes of blinded unknowns were then used to quantify each cytokine by inverse regression.

### **Paired difference *t*-test for comparing cytokine secretion levels**

A paired difference *t*-test was used to test for statistical significance when comparing cytokine levels between control and stimulated cells and also between T cell subsets. As indicated in Figure 4, significance was noted if the null hypothesis (“the cytokine levels of the two cell types in question are equal”) could be rejected based on the paired *t* value calculated from:

$$t = \frac{\bar{x} - \Delta}{s/\sqrt{n}}$$

where  $\bar{x}$  is the mean difference between initial slopes (as compared for each ring individually),  $\Delta$  is the hypothesized difference (in this case 0 since testing for any difference),  $s$  is the standard deviation of the difference, and  $n$  is the sample size (number of independent ring sensing elements used, in this case 4 or 5 per cytokine). To calculate  $\bar{x}$  and  $s$ , the difference between initial slopes was calculated for each ring. The *t* value was compared to the Student’s *t* distribution with  $n-1$  degrees of freedom to determine significance at 95% or 99% confidence levels. A one-tailed *t* test was used in all cases based on 1) prior knowledge of Th1 and Th2 cytokine signatures and 2) the fact that stimulated cells secrete more cytokines.

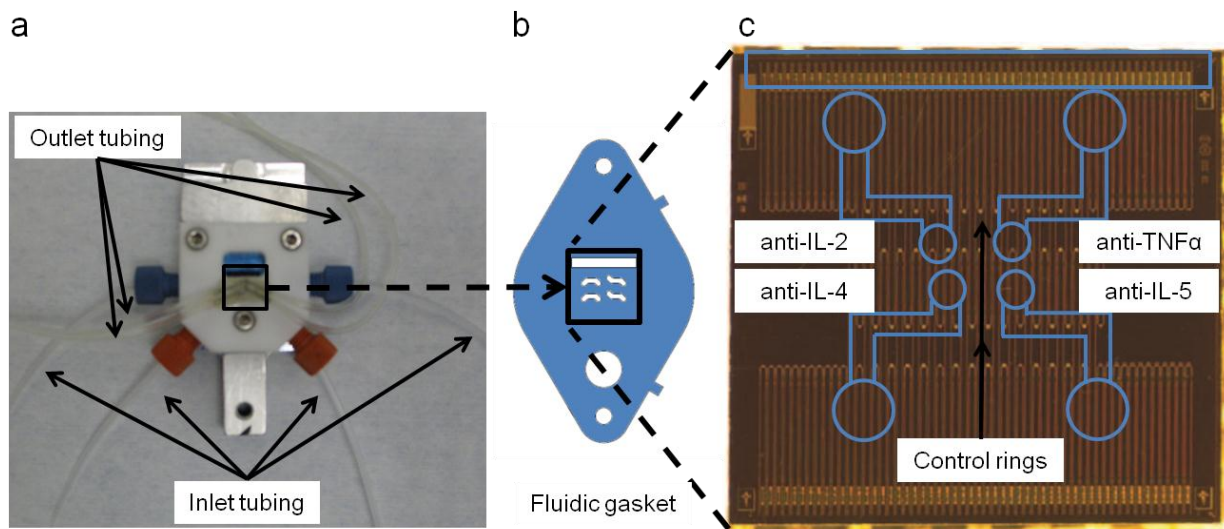


**Figure S1. Ring resonator chip micrograph with microfluidic schematic.** (a) Photograph of 4-channel microfluidic cartridge and housing for ring resonator chip. The chip (outlined by black square) is seated on an aluminum chip holder and covered with a white Teflon flow cartridge with 4 independent microfluidic channels, 4 inlet ports, and 4 outlet ports. Each inlet tube is placed in a separate antibody solution for chip functionalization, and the outlet tubes are connected to syringes operated in withdraw mode that generate solution flow via negative pressure. (b) A 0.007''-thick 4-channel laser-cut Mylar gasket that is placed between the chip and the flow cartridge directs solution to one of 4 groups of rings. (c) Each channel covers 4-6 sensor rings and 2 temperature control rings, with minor variations in alignment between different gaskets. This allows creation of a 4-plex chip (6 mm<sup>2</sup>) for simultaneous detection of IL-2, IL-4, IL-5, and TNF $\alpha$  with 4-6 redundant measurements each. Rings that are covered by the gasket during antibody functionalization (as noted by the black arrows) are not modified with antibody and serve as controls in subsequent experiments. Access to waveguide grating couplers for optical insertion is permitted by the rectangular opening in the gasket over the top of the chip.

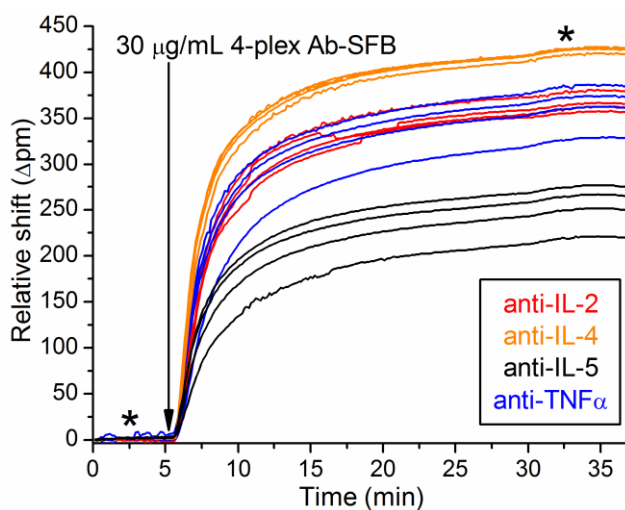


**Figure S2. Real-time plot of 4-plex capture antibody loading.** Using the microfluidics described in Figure S1, covalent modification of the rings with 4 capture antibodies (Abs) can be observed in real time. As indicated, 30  $\mu\text{g mL}^{-1}$  of each of 4 Abs modified with an aldehyde moiety (4-formyl benzamide) can react with hydrazine functionalities introduced to the surface of the rings through silanization. Aniline catalyzes the hydrazone bond formation that provides covalent antibody loading.<sup>3,6</sup> It was found that 200-400 pm of antibody coverage (3-6  $\text{ng mm}^{-2}$ )<sup>4</sup> gives optimal performance. \* indicates 100 mM PBS pH 6 + 50 mM aniline running buffer, which was flowed before and after antibody loading to provide a net shift.

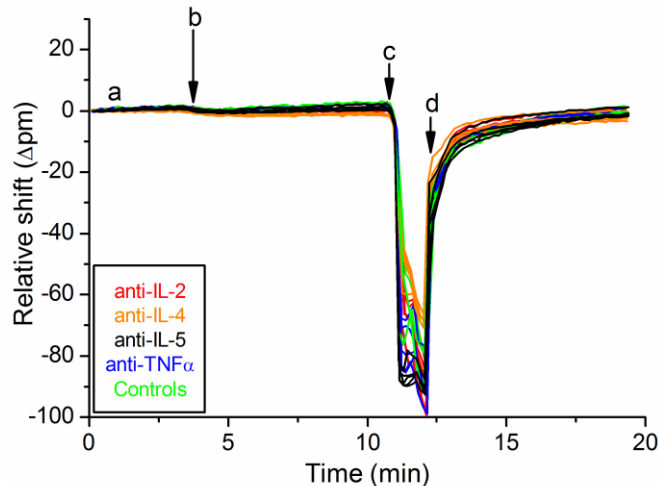


**Figure S3. Negative control experiment for one-step sandwich assay.** There is no signal associated with flowing cell media (RPMI 1640 + 10% FBS) containing the 4 detection antibodies without any cytokines. After flowing cell media (**a**) to establish a baseline, the introduction of cell media with  $1 \mu\text{g mL}^{-1}$  of each of 4 detection antibodies (**b**) results in no appreciable response. A 10 mM glycine pH 2.2 rinse (**c**) is used to regenerate the surface prior to switching back to cell media (**d**) for a return to the original baseline.<sup>1,7</sup> Control rings in green are not functionalized with any capture antibodies (Figure S1) but are blocked along with the other rings.

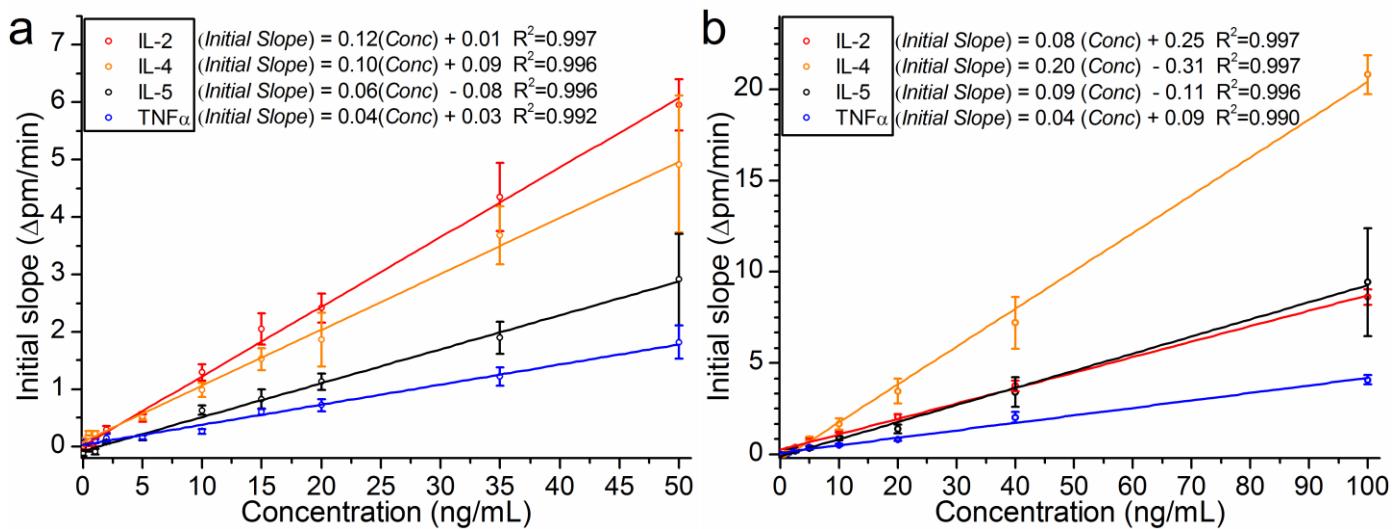


**Figure S4. Calibration curves for quantitative multiplexed analysis.** The average control-ring corrected initial slope is plotted as a function of cytokine concentration for each of 4 cytokines. All multiplexed standards were prepared in cell culture media containing 10% serum, and all calibration data was obtained on a single chip that was also used for determination of unknowns. Each calibration curve is fit well with a linear regression (all  $R^2 > 0.990$ ), and the displayed equations are used to quantitate solutions with unknown cytokine concentrations via inverse regression. (**a**) The calibration curves for blinded unknown determination (Table S1a) used 10 standards between 0 and  $50 \text{ ng mL}^{-1}$  while (**b**) the calibration curves for cell culture studies (Table S1b) used 7 standards between 0 and  $100 \text{ ng mL}^{-1}$ . Minor variations in calibration curve slopes between (**a**) and (**b**) and also between different cytokines are due to different amounts of capture antibody loaded during initial chip functionalization and variable antibody kinetics, respectively. Error bars represent the standard deviation of the initial slope for  $n=4-6$  rings.



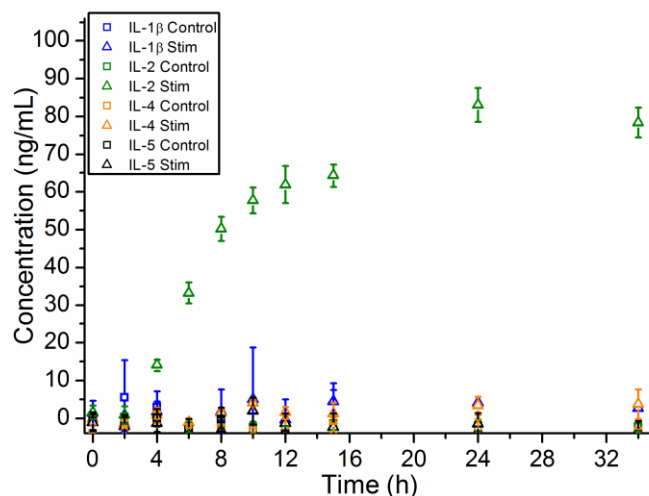


**Figure S5. 4-plex cytokine temporal secretion profile for Jurkat T cells.** Control ( $\square$ ) and stimulated ( $\Delta$ ) aliquots taken from Jurkat T cell cultures ( $10^6$  cells  $\text{mL}^{-1}$ ) at several time points over 1.5 days were analyzed by one-step sandwich immunoassays. One-step sandwich immunoassays allow better time resolution (2 h) than two-step assays. As expected, Jurkat T cells secrete only IL-2 and only when stimulated with PMA and PHA.<sup>8,9</sup> Error bars represent the total propagated standard error that includes: (1) the variation in  $n=3-6$  rings used to analyze cytokine levels and (2) the linear regression error resulting from fitting the calibration curve. These results were validated by ELISA (Figure S6).

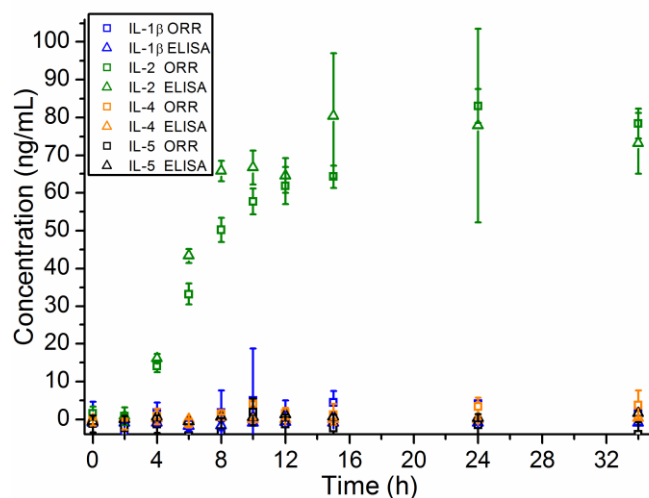


**Figure S6. ELISA validation of temporal secretion study.** Aliquots taken from Jurkat T cell cultures ( $10^6$  cells  $\text{mL}^{-1}$ ) at several time points following PMA/PHA stimulation were analyzed by (1) one-step sandwich immunoassays using optical ring resonators ( $\square$ , ORR in legend) and (2) a set of four commercial ELISAs ( $\Delta$ ). The four ELISAs [IL-2 (BD OptEIA 550611, BD Biosciences), IL-4 (88-7046, eBioscience), IL-5 (88-7056, eBioscience), and IL-1 $\beta$  (88-7910, eBioscience)] were run in parallel according to the manufacturer's instructions to validate the results of the one-step sandwich assays. These ELISA kits utilized the same antibody clones as those used for ring resonator assays. ELISA results show strong agreement with ORR results for all cytokines tested; only IL-2 secretion was observed at appreciable levels. Error bars for ORR data represent the total propagated standard error that includes: (1) the variation in  $n=3-6$  rings used to analyze cytokine levels and (2) the linear regression error resulting from fitting the calibration curve. ELISA error bars represent the standard deviation for triplicate absorbance measurements.

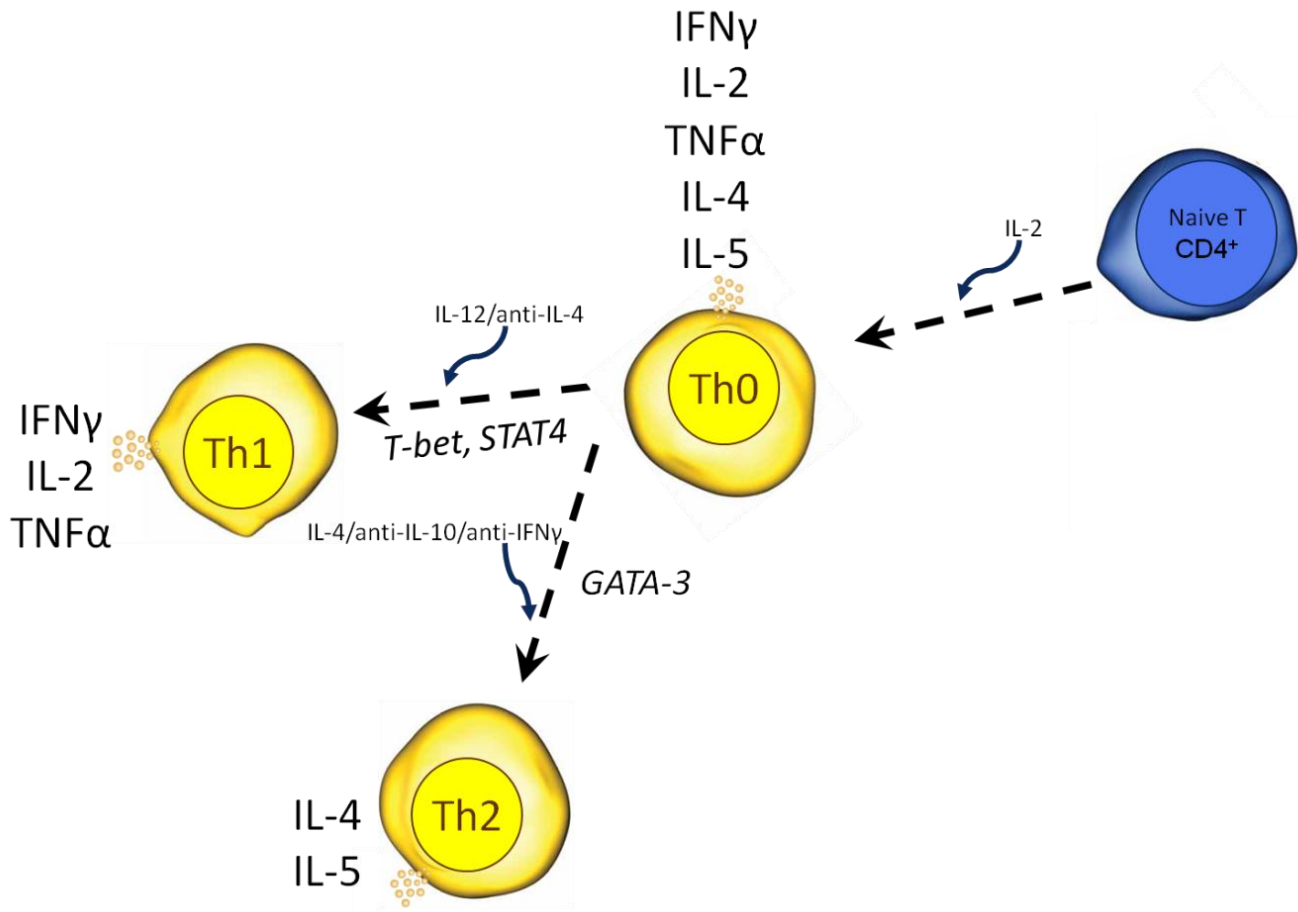


**Figure S7. T cell differentiation schematic and cytokine secretion signatures.** This schematic summarizes the differentiation cues (curved blue arrows), relevant pathways (italicized under dashed black arrows), and cytokine secretion signatures for Th0, Th1, and Th2 cell differentiation paths.<sup>10-13</sup> Naïve CD4<sup>+</sup> T cells isolated from donor blood can be activated to the Th0 subset with IL-2. Th0 cells can secrete both Th1 and Th2 cytokines, while Th1 and Th2 cells have unique signatures. Over a period of weeks or even months in culture, a large portion of T cells are known to remain undifferentiated or as Th0.<sup>14</sup> The cytokine signatures displayed include the hallmark cytokines but are not exhaustive of all cytokines secreted by each subset.

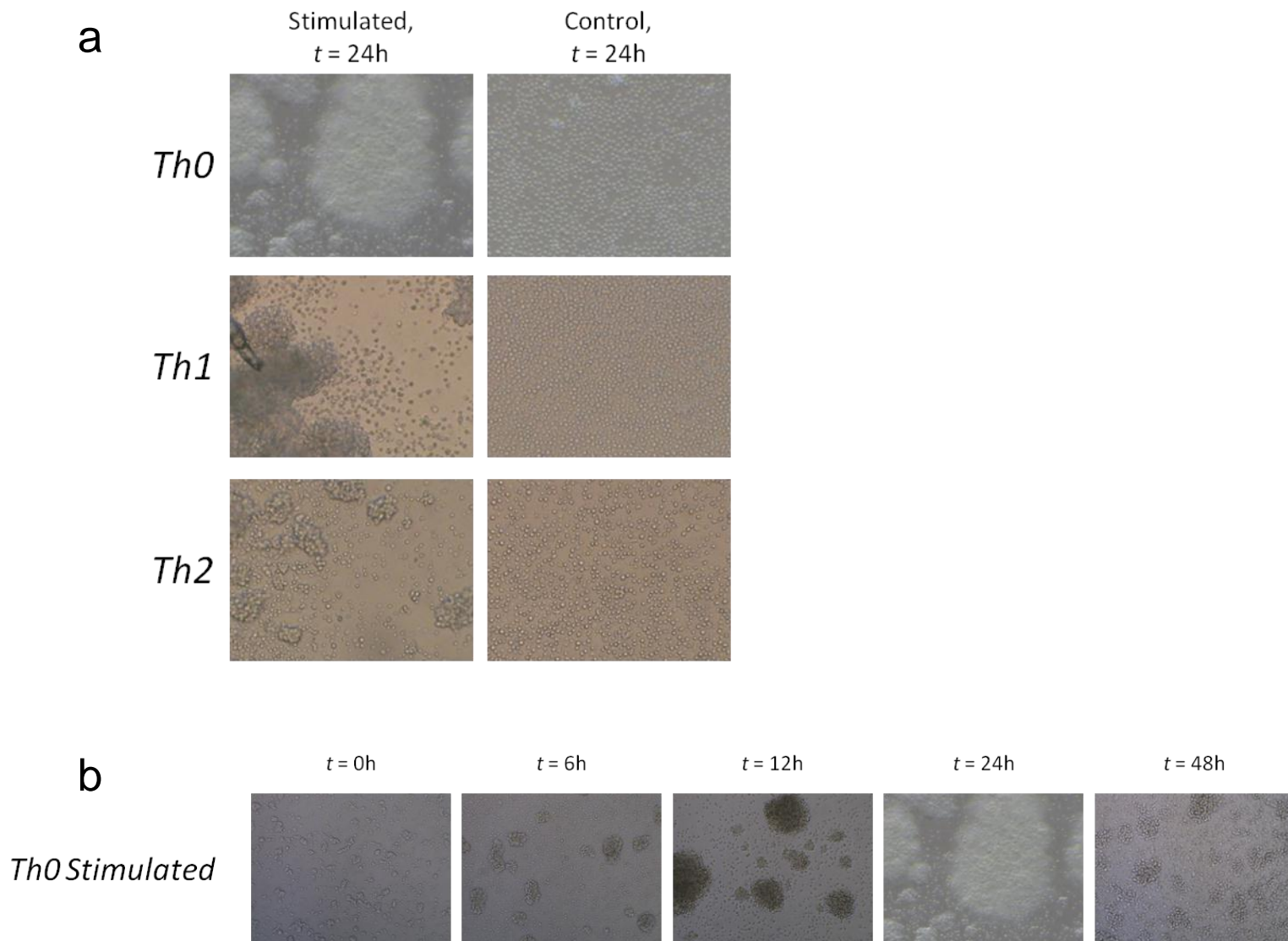


**Figure S8. Primary T cell microscope images: Time-course study.** (a) T cell subsets (both control and PMA/ionomycin-stimulated) were cultured for 24 h at the following cell densities: Th0 =  $4.3 \times 10^6$  cells  $\text{mL}^{-1}$ , Th1 =  $1.9 \times 10^6$  cells  $\text{mL}^{-1}$ , Th2 =  $1.0 \times 10^6$  cells  $\text{mL}^{-1}$ . As expected, stimulated cells consistently display much greater cell aggregation. (b) Aggregation was also demonstrated to increase over time for stimulated Th0 cells at  $2.8 \times 10^6$  cells  $\text{mL}^{-1}$ . Significant aggregation was evident after only 6 h, and by 48 h almost all cells existed in aggregates. All images were acquired at 200x total magnification.

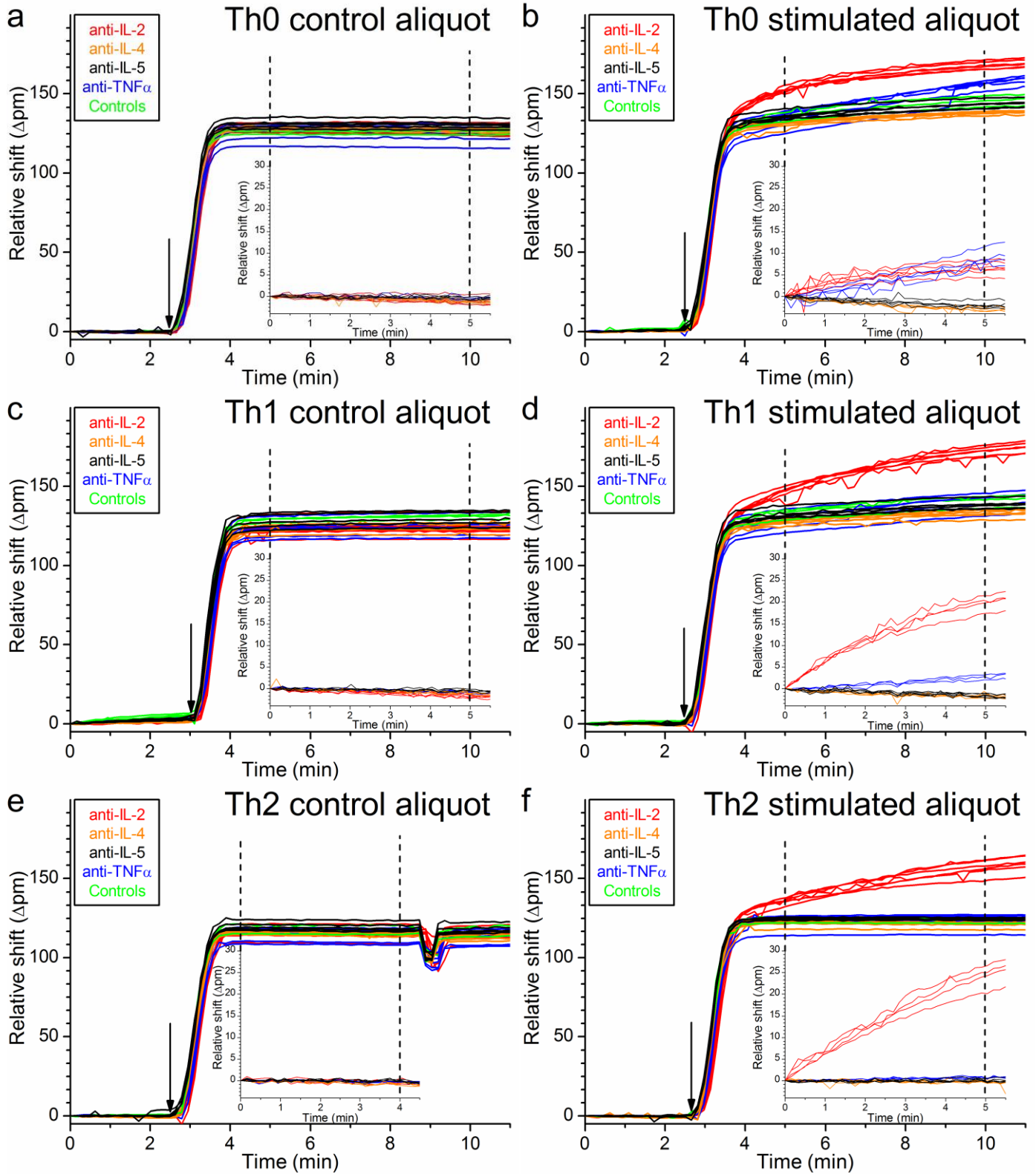


**Figure S9. Real-time multiplexed cytokine binding for Th0/Th1/Th2 culture aliquots.** Aliquots were taken from both control and PMA/ionomycin-stimulated T cell subsets (7-day activation and differentiation followed by 24-h stimulation).<sup>14,15</sup> Cell-free aliquots spiked with 4 cytokine detection antibodies were flowed across a single chip in a series

of one-step sandwich assays for (a) Th0 control, (b) Th0 stimulated, (c) Th1 control, (d) Th1 stimulated, (e) Th2 control, and (f) Th2 stimulated aliquots. Sterile cell media was used as a running buffer prior to addition of each aliquot at  $t = 2-3$  min (signified by the black arrow in each plot). An immediate bulk refractive index (RI) shift of  $\sim 125$  pm was observed on all rings for all aliquots due to  $\sim 1\%$  dimethyl sulfoxide (DMSO) present in the aliquots (owing to PMA, ionomycin, and protease inhibitors each added as DMSO solutions, with pure DMSO substituted for PMA and ionomycin in control aliquots for consistency). Following the bulk RI shift, multiplexed cytokine binding was quantified by measuring the initial slope of the real-time data plot for each ring. The black dashed lines in each plot signify the range of data used to calculate initial slopes. The insets in each plot show control ring-corrected data on which linear regressions were performed prior to calibration with cytokine standards. In each case, control cells show little to no cytokine binding compared to stimulated cells. The cytokine levels quantified for these T cell aliquots, normalized to the number of cells per unit volume, are displayed in Figure 4.

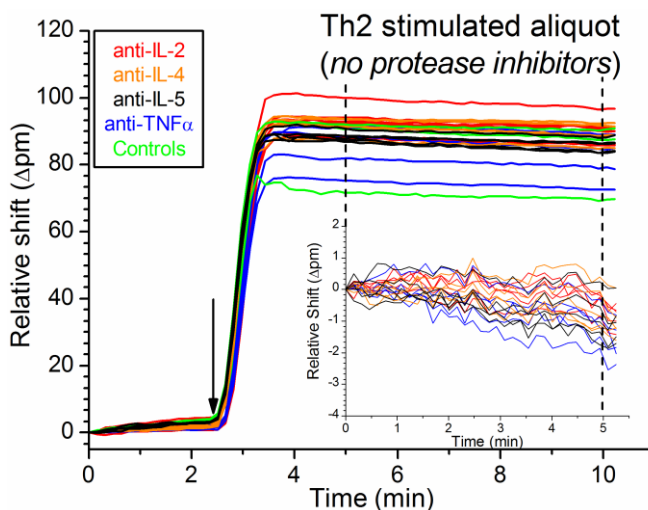


**Figure S10. Effect of proteases on real-time binding curves.** It was observed that cell culture secretion aliquots demonstrate significant protease activity, as shown above by the negative slope on all rings when no protease inhibitors are added. Aliquots were taken from PMA/ionomycin-stimulated T cell subsets (7-day activation and differentiation followed by 24-h stimulation). Cell-free aliquots spiked with 4 cytokine detection antibodies were run over the chip in a one-step sandwich assay. Only the Th2 stimulated aliquot is shown as a representative example, but all aliquots from all T cell subsets tested showed a similar downward sloping response due to proteases. Sterile cell media was used as a running buffer prior to addition of each aliquot at  $t = 2.5$  min (signified by the black arrow). An immediate bulk RI shift of  $\sim 90$  pm was observed on all rings due to  $\sim 0.7\%$  dimethyl sulfoxide (DMSO) present in the aliquots (owing to PMA and ionomycin added as DMSO solutions). Following the bulk RI shift, multiplexed cytokine binding could not be quantified by measuring the initial slope because of the high protease background. The black dashed line signifies the range of data used to calculate initial slopes, with the inset displaying the control ring-corrected plots. Since the addition of protease inhibitors remedied the negative sloping background (Figure S9f), the negative slope depicted is likely due to protease activity on the blocking proteins and capture antibodies bound to the microrings.

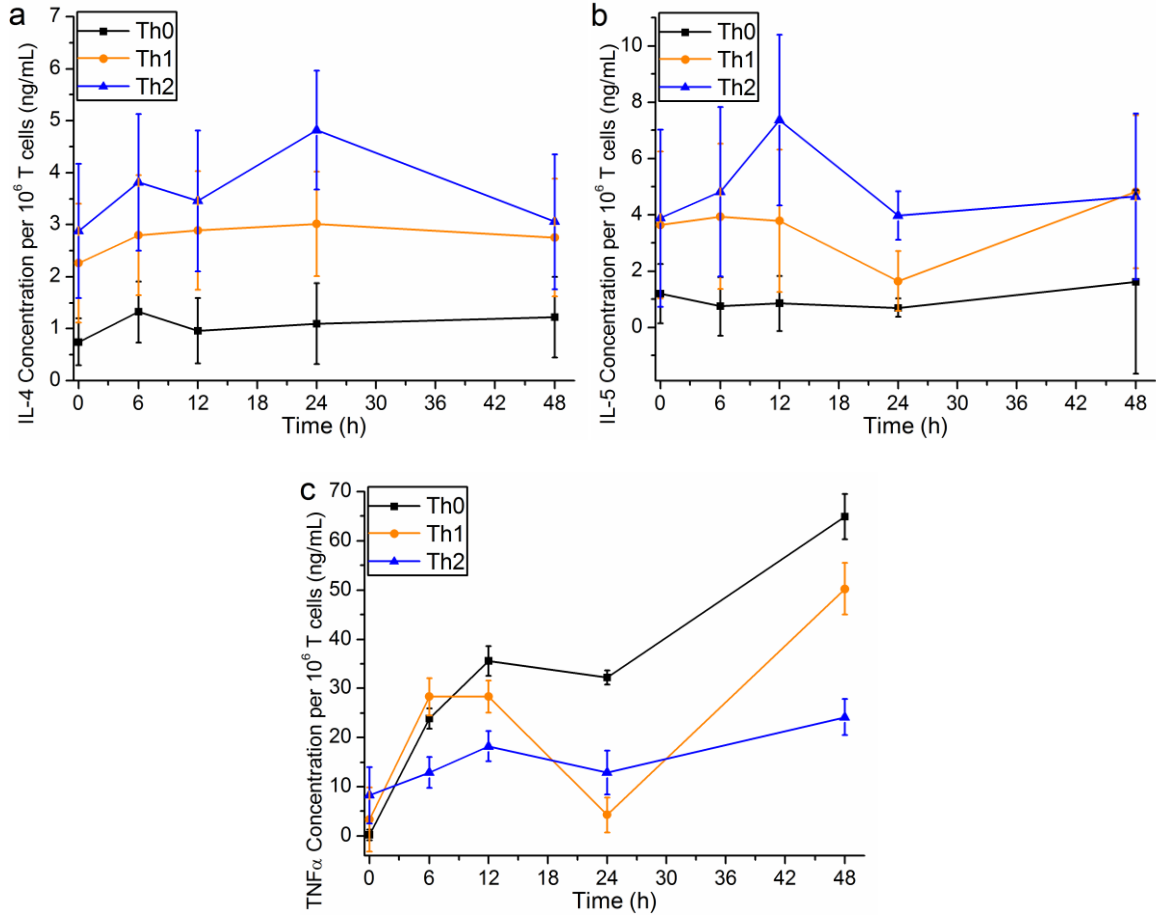


**Figure S11. Cytokine temporal secretion profiles for Th0, Th1, and Th2 subsets.** Aliquots taken from T cell cultures at several time points following stimulation were analyzed by one-step sandwich immunoassays. IL-4 (a), IL-5 (b), and TNF $\alpha$  (c) temporal secretion levels for stimulated Th0, Th1, and Th2 subsets are shown (temporal profiles of IL-2 are shown in Figure 5 of the main text). All concentrations are normalized to the number of cells per unit volume in each culture (per  $10^6$  cells  $\text{mL}^{-1}$ ). Error bars represent the total propagated standard error that includes: (1) the variation in  $n=3-5$  rings used to analyze each cytokine and (2) the linear regression error resulting from fitting the calibration curve.

<b>a</b> Standard	<i>Volume added (<math>\mu\text{L}</math>)</i>					
	RPMI + 10% FBS...	Detection Ab cocktail	IL-2	IL-4	IL-5	TNF $\alpha$
1	431	4	50	5	10	0
2	439	4	35	2	20	0.5
3	439	4	20	1	35	1
4	464	4	15	0.5	15	2
5	431	4	10	0	50	5
6	466	4	5	15	0	10
7	444	4	2	35	0.5	15
8	450	4	1	20	5	20
9	410	4	0.5	50	1	35
10	434	4	0	10	2	50

<b>b</b> Standard	<i>Volume added (<math>\mu\text{L}</math>)</i>					
	RPMI + 10% FBS...	Detection Ab cocktail	IL-2	IL-4	IL-5	TNF $\alpha$
1	441	4	40	5	10	0
2	452	4	20	2.5	20	1.25
3	442	4	10	1.25	40	2.5
4	485	4	5	0	1.25	5
5	461	4	2.5	20	2.5	10
6	465	4	1.25	10	0	20
7	411	4	0	40	5	40

**Table S1. Calibration standard cocktails.** Multiplexed cytokine calibration standards utilized for one-step sandwich assays for (a) unknown determination shown in Figure 3 and (b) T cell culture secretion analyses shown in Figure 4 and Figure 5. Each standard is prepared in the same cell media as that used for T cell culture and spiked with 1  $\mu\text{g}/\text{mL}$  of each detection antibody (4  $\mu\text{L}$  of cocktail containing 125  $\mu\text{g mL}^{-1}$  of each detection antibody). All cell culture standards in (b) were prepared and stored in the same manner as cell culture aliquots: stored overnight at  $-20\text{ }^{\circ}\text{C}$  when applicable and spiked with detection antibody at the same time as cell samples. Each set of standards contains a negative control (0  $\text{ng mL}^{-1}$ ) standard for each cytokine.

<i>Cytokine</i>	<i>Molecular weight</i> (kDa)	<i>Limit of detection</i>	
		<i>Mass per volume</i> (ng mL <sup>-1</sup> )	<i>Molar</i> (pM)
IL-2	15	1.9	119
IL-4	15	1.0	67
IL-5	14*	3.6	80*
TNF $\alpha$	17**	4.6	88**

**Table S2. Limits of detection: One-step sandwich.** The limit of detection (LOD) used herein is based on the traditional analytical chemistry definition: the concentration that corresponds to the negative control signal (initial slope for 0 concentration of particular cytokine in presence of other cytokines, detection antibodies, and cell media) plus 3 standard deviations. LODs were calculated for each cytokine in terms of both mass per unit volume (ng mL<sup>-1</sup>) and molarity (pM). The LODs showed remarkable similarity, especially in terms of molarity, with all detection limits around 100 pM. These LOD values, though slightly inferior to LODs obtained in cell media for two-step sandwich assays (generally 0.5 - 1.0 ng mL<sup>-1</sup>),<sup>7</sup> are still sufficient to conduct cell secretion assays performed herein and greatly reduce the time required to perform assays.

\* indicates that IL-5 (monomeric molecular weight = 14 kDa) exists as a glycosylated homodimer, which alters the molar LOD. The molar LOD used here is assuming IL-5 glycosylated homodimer (~45 kDa total molecular weight).<sup>16</sup>

\*\* indicates that TNF $\alpha$  (monomeric molecular weight = 17 kDa) exists as a homotrimer. The molar LOD used here is assuming TNF $\alpha$  homotrimer (52 kDa total molecular weight).<sup>16</sup>



## Supporting Information References

- (1) Washburn, A. L.; Gunn, L. C.; Bailey, R. C. *Anal. Chem.* **2009**, *81*, 9499-9506.
- (2) Byeon, J.-Y.; Bailey, R. C. *Analyst* **2011**, *136*, 3430-3433.
- (3) Byeon, J.-Y.; Limpoco, F. T.; Bailey, R. C. *Langmuir* **2010**, *26*, 15430-15435.
- (4) Luchansky, M. S.; Washburn, A. L.; Martin, T. A.; Iqbal, M.; Gunn, L. C.; Bailey, R. C. *Biosens. Bioelectron.* **2010**, *26*, 1283-1291.
- (5) Michie, C. A.; McLean, A.; Alcock, C.; Beverley, P. C. L. *Nature* **1992**, *360*, 264-265.
- (6) Dirksen, A.; Dawson, P. E. *Bioconj. Chem.* **2008**, *19*, 2543-2548.
- (7) Luchansky, M. S.; Bailey, R. C. *Anal. Chem.* **2010**, *82*, 1975-1981.
- (8) Manger, B.; Hardy, K. J.; Weiss, A.; Stobo, J. D. *J. Clin. Invest.* **1986**, *77*, 1501-1506.
- (9) Weiss, A.; Wiskocil, R.; Stobo, J. *J. Immunol.* **1984**, *133*, 123-128.
- (10) Ansel, K. M.; Lee, D. U.; Rao, A. *Nat. Immunol.* **2003**, *4*, 616-623.
- (11) Murphy, K. M.; Reiner, S. L. *Nat. Rev. Immunol.* **2002**, *2*, 933-944.
- (12) O' Garra, A. *Immunity* **1998**, *8*, 275-283.
- (13) Zhu, J.; Yamane, H.; Paul, W. E. *Annu. Rev. Immunol.* **2010**, *28*, 445-489.
- (14) Cousins, D. J.; Lee, T. H.; Staynov, D. Z. *J. Immunol.* **2002**, *169*, 2498-2506.
- (15) Yano, S.; Ghosh, P.; Kusaba, H.; Buchholz, M.; Longo, D. L. *J. Immunol.* **2003**, *171*, 2510-2516.
- (16) Haddad, J. J. *Biochem. Biophys. Res. Commun.* **2002**, *297*, 700-713.